Evaporative purification to produce highly monodisperse polymers:
Application to polystyrene for $n = 3$–13 and quantification of T_g from oligomer to polymer

S. Zhu,[1] Y. Chai,[1] and J. A. Forrest[1,2,*]

[1]*Department of Physics and Astronomy, University of Waterloo, Waterloo, ON, Canada N2L 3G1*
[2]*Perimeter Institute for Theoretical Physics, 31 Caroline St., Waterloo, ON, Canada N2L 2Y5*

We demonstrate the use of selective thermal evaporation to separate and purify small molecular weight polymers into highly monodisperse polymers over an extended range of polymerization index. By exploiting the calculated dependence of polymer vapor pressure on polymerization index N and temperature T, we can isolate individual components (N-mers) of an initially polydisperse mixture. To demonstrate this ability, we consider polystyrene samples of $M_w = 600$ g/mol and $M_w = 890$ g/mol with narrow molecular weight distributions, as well as a $M_w = 1200$ g/mol sample with a broader distribution. In each case we are able to separate the sample into milligram quantities of many different components. Using this technique, we have been able to isolate N-mers from 3 to 13. We use differential scanning calorimetry to measure the T_g values of these components, and find that the components have the same T_g values independent of the M_w or polydispersity of the sample they originate from. We find that even initially narrow molecular weight distributions have many different components whose T_g values can differ by more than 50 K. Calculations suggest the isolated components have M_w/M_n values less than 1.001 and through a second iteration of the process could become as low as 1.000 003. The measured T_g values for the N-mers as well as large N polymers are well described by a simple relation derived from the Fox equation for the T_g of mixtures.

I. INTRODUCTION

Arguably, the most important single parameter describing a polymer is the polymerization index, N. Many different physical properties of polymers, such as the glass transition temperature, T_g [1], and dependence of T_g on polydispersity [2], viscoelasticity [3], solubility [4], and miscibility with other polymers [5], can depend strongly on the polymerization index. An excellent discussion of the importance of the polymerization index is provided in Ref. [6]. It is for relatively small values of N that there is the greatest change in properties as N increases, and the materials make the transition from being oligomeric to polymeric. In comparisons between theoretical and experimental determinations of the order-disorder transition in block copolymer melts, even modest polydispersities were shown to give rise to significant differences [7]. Any method of producing polymers will result in a distribution of the polymerization index. The polydispersity index, PDI $= M_w/M_n$, provides a metric to quantify how monodisperse a particular distribution of molecules is. For a completely monodisperse sample (i.e., all of the molecules have exactly the same value of N), the PDI is identically equal to 1. Most common methods for producing polymers lead to PDI values significantly greater than 1. In contrast, naturally produced biopolymers have PDIs extremely close to unity, but are restricted to proteins, and not to a wide range of polymers. While free radical polymerization produces polymers with a PDI in the range 1.5–2, living polymerization [8] can produce a wide range of polymers usually with a Poisson distribution of N and PDI values relatively close to unity. Practically, PDI values ~1.01 are considered to be very monodisperse. However, a simple example can show how misleading this criterion can be. For example, consider a low M_w sample of polystyrene (PS) where the composition of the sample is 25% $N = 5$, 50% $N = 6$, and 25% $N = 7$. In this case calculation reveals a M_n value of 600 g/mol and a PDI value of 1.01 even though the sample is only 50% made up of the polymer suggested by the M_n value. While this example is somewhat artificial, a more realistic example is given by matrix-assisted laser desorption ionization measurements of polystyrenes produced by living polymerization [9]. In those studies, a PS with $M_n = 2400$ g/mol and $M_w/M_n = 1.04$ exhibited 19 different N-mer components. It is certainly notable that living polymerization to produce these fairly monodisperse materials is a nontrivial technique requiring significant experience and expertise in synthetic chemistry.

The importance of studying the effect of polymerization index on physical properties and the resulting necessity for highly monodisperse systems—pure N-mers—has been recognized [2,7,10–14]. While monodisperse n-alkanes have been studied often, the same is not true of other polymers. For polystyrene, a number of studies have involved fractionation of polymerized materials into more monodisperse samples. Typically, vacuum distillation is used to isolate the dimers or trimers, and other techniques such as liquid chromatography [10] or solvent fractionation is employed for larger molecular weights. It remains a challenge to obtain macroscopic quantities of N-mers for larger N in a way that is applicable to a wide range of polymer systems. It is also clear that the fractionated components of some of these studies are also not simple N-mers, but blends as well [11].

As is the case for aliphatic chain molecules [15], polymers have non-negligible vapor pressure for small values of N. For larger values of N, temperatures required for significant vapor pressure are usually greater than those necessary for thermal degradation. Both of these cases can be seen in previous studies

_____

*jforrest@uwaterloo.ca

incorporating thermal evaporation of polymers [16–19]. For the case of polystyrene, the polymer we employ as an example, thermal decomposition is found to occur at temperatures near 570 K [20]. This is a relatively low temperature for thermal deposition, and for this reason, as well as the simplicity of solvent based spin coating deposition techniques, thermal evaporation of polymers has remained to a large extent, unexploited. Purification by evaporation is among the oldest of scientific techniques. In fact, Aristotle is said to have written about it in his "Meteorologica." Distillation of water was first described almost 2000 years ago [21]. Distillation is often applied to cases where the vapor pressures are approaching atmospheric pressure and so these distillation techniques are most commonly applied to more volatile materials. In cases where the vapor pressures are not as large, vacuum distillation techniques are often employed. For materials unstable at high temperatures, short path distillation or even molecular distillation (where the distillation path is similar to the molecular mean free path) is a preferred technique [22]. This group of techniques is commonly employed for molecular distillation in both laboratories and industry. It would seem possible that distillation techniques should be applicable for polymers significantly beyond the parameter range where it is currently employed. Below we develop a numerical simulation based on available data intended to demonstrate feasibility and limits of monodispersity. From there we describe our experimental apparatus, and the characterization of the N-mer specimens collected. In particular, we measure the T_g values of the N-mers, and use that data as well as data for higher M_n samples, to provide a single free parameter semiempirical relation that describes the $T_g(N)$ values from $N = 3$ to $N \to \infty$.

II. NUMERICAL STUDIES

Consider a mixture of pure N-mers, with the amount of component with k monomers as n_k, and the vapor pressure of that component as P_k. We can use the mass transport relation of Langmuir [23], as well as Raoult's law [24] for vapor pressures of mixtures to obtain the following set of coupled equations determining the mass transport:

$$\frac{dm_k}{dt} = \alpha \frac{n_k}{\sum n_k} P_k \frac{\sqrt{k}}{\sqrt{T}}, \qquad (1)$$

where m_k is the mass of component k, $\frac{n_k}{\sum n_k}$ is the mole fraction of the kth, N-mer, and α is a constant that depends on experimental conditions and the monomer molecular weight. For these simulations, α determines the time scale of the mass loss. In order to effectively use these equations, knowledge of the vapor pressure of pure N-mers is required. Since the vapor pressure of pure N-mers of polystyrene have not been measured, we calculate model values for our simulation. To do this we employ the lattice fluid theory of Sanchez *et al.* [25,26]. In the lattice fluid theory of a polymer melt [25], the equation of state is written as

$$\tilde{\rho}^2 + \tilde{P} + \tilde{T}\left[\ln(1 - \tilde{\rho}) + \left(1 - \frac{1}{r}\right)\tilde{\rho}\right] = 0, \qquad (2)$$

where r is the number of lattice sites taken by the N-mer (and is not necessarily the same as the polymerization index), $\tilde{T}$ is a reduced temperature, $\tilde{P}$ a reduced pressure, and $\tilde{\rho}$ a
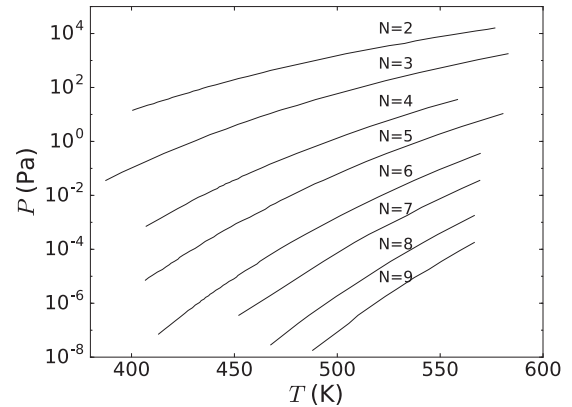

FIG. 1. Calculated vapor pressures for polystyrene N-mers as a function of temperature and polymerization index, N, using Ref. [25] and the parameters from Ref. [26].

reduced density. The conversion of these reduced quantities to real physical values uses microscopic parameters for that particular fluid. The relevant values are found in Ref. [26]. The values of P,T which result in equal minimum values of the Gibbs free energy for the liquid and vapor phases define the liquid vapor coexistence curve that can be used to find the polymer vapor pressure. We note that in the limit of $r \to \infty$ the vapor pressures vanish, and so it is not obvious that there will be enough contrast for increasing N. While the actual values may not be quantitatively accurate, especially because the end groups are not considered at all in the calculation, we expect the N dependence to provide a good guide for our own experimental process. Figure 1 shows the calculated vapor pressures as a function of T and polymerization index N for polystyrene and N values between 2 and 9. In Fig. 1 it is evident that for these values of N, there is significant enough dependence of vapor pressure on N for purification by evaporation.

With these values for $P_k(T)$ and Eq. (1), we can simulate the process of separation by evaporative deposition. To do this, we start at some temperature (usually 400 K in the experiments) and collect the products of evaporation. In the simulation, this is done by integrating Eq. (1) over some time interval. For all temperatures, the common value of α determines the time scale for the simulation. When the rate of deposition falls below some value, we increase the temperature by 20 K and repeat the process to collect the next N-mer. The reason for the 20 K increase in temperature is that this is approximately the temperature increase required to get an order of magnitude change in the temperature-dependent vapor pressure. At each temperature, we wait some time before starting collection. This step ensures that all material of smaller N values has been exhausted as much as possible. The results of this simulated process are shown in Fig. 2. In this figure we start with the distribution of N-mers labeled "initial," and by collecting at each temperature, are able to arrive at the evaporatively purified components shown for each temperature. We can see that at each collection temperature the vast majority of product is a single value of N with less than 5% of $N + 1$ impurity. While the initial distribution has 11 components and a $M_w/M_n \sim 1.2$, these resulting purified products have at most three measurable
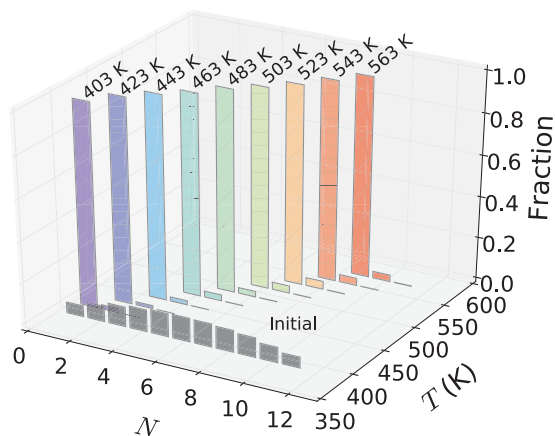
FIG. 2. Initial distribution of monomers, and products after simulated evaporative purification method described in the text.

components, and a polydispersity index $M_w/M_n < 1.001$. Further simulation using one of the products of Fig. 2(b) as a starting material leads to a $M_w/M_n \sim 1.000\,003$. More importantly, the simulations reveal only a very weak dependence of the final product composition on the starting composition. We have also preformed simulations under isothermal condition, and we find that the simulations suggest that at a constant temperature we can still deposit monodisperse N-mers, but the time range required is prohibitive.

III. EXPERIMENTAL TECHNIQUE

We have tested the technique experimentally using a series of polystyrene samples. We have employed PS with $M_w = 600$ g/mol, $M_w/M_n = 1.2$ and $M_w = 890$ g/mol, $M_w/M_n = 1.12$, both from Polymer Source Inc., and $M_w = 1200$ g/mol, $M_w/M_n \sim 1.6$ from Scientific Polymer Products. For each polymer, a sample was placed on a flat substrate—usually a polished Si wafer of 0.3 mm thickness—onto the hot stage of a Linkam hot stage which was placed inside a vacuum chamber. The collecting substrate is separated from the deposition source by thermally insulating spacers of about 3 mm. The chamber is evacuated with an Agilent Technologies SH-110 dry scroll pump to a pressure of approximately 0.3 mbar. Once the pressure reaches this minimum value, a small amount of nitrogen gas is admitted to the chamber until the ambient pressure is about 1–3 mbar. This small pressure of gas facilitates heat exchange and improves the temperature stability and ability to separate different N-mers. The same temperature and collection procedure used in the simulation was then applied to this real material, and the deposition products collected for 120-min intervals. The mass of each deposition was recorded and then the material was pressed into a sample pan and differential scanning calorimetry was performed with a Q100 DSC instrument by TA instruments with a heating/cooling rate of 10 K/min.

IV. EXPERIMENTAL RESULTS AND DISCUSSION

A. Separating N-mers

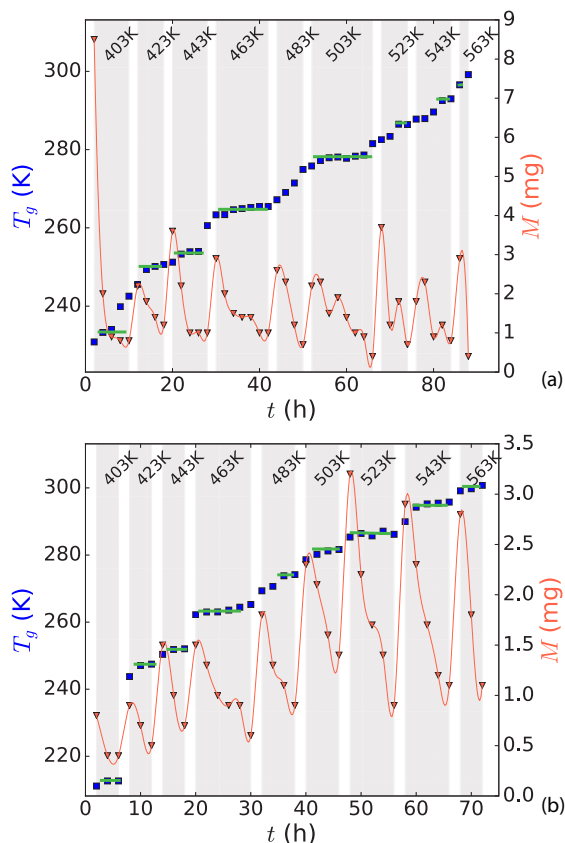Figure 3 shows the processing temperature and deposition product mass as well as measured T_g values for the $M_w =$

FIG. 3. Measured deposited mass (triangles) and T_g values (squares) of evaporatively isolated components of N-styrene. The starting polymers in this case are $M_w = 600$ g/mol (top) and $M_w = 890$ g/mol (bottom).

600 g/mol and the $M_w = 890$ g/mol polystyrene. The T_g values plotted are the T_g values of *only* the material collected in that time interval (each of which is 2 h), and not the T_g of the integrated deposition at that temperature. The reason for this distinction is important. During a deposition there are time-dependent changes in the composition of the evaporated material, and hence the deposited film. If we are in a situation where we have already deposited most of a particular N-mer, then when we change temperature to deposit the $N + 1$-mer, the initial part of that deposit may still contain some of the N-mer. If we continue to deposit at the same temperature over much larger times, then at some point we will have exhausted most of the $(N + 1)$-mer, and will start to deposit an appreciable amount of the $(N + 2)$-mer. Since the different N-mers have significantly different vapor pressures, then at any temperature if we consider the $T_g(t)$ during deposition, we should expect to see a plateau in T_g corresponding to a particular value of N. Such plateaus are readily evident in Fig. 3 for most of the starting compositions and at most of the temperatures. We note that for both the $M_w = 600$ g/mol and $M_w = 890$ g/mol PS samples, the same N-mer is collected at the same deposition temperature. Only the 483 K evaporation failed to yield a well-defined plateau in the T_g value for the $M_w = 600$ g/mol polymer. In a more refined process, one might imagine using a quartz crystal microbalance sensor to monitor the rate of deposition concurrently, and use that to

determine the optimum time intervals to collect for pure N-mer isolation.

A similar process was carried out with the $M_w = 1200$ g/mol PS. In this case, we were also able to measure plateaus in the T_g value of the deposited polymer, and (as will be evident below) the individual T_g values of N-mers are the same as those for the original samples in Fig. 3—indicating the same N-mers are being isolated. However, the temperature at which a particular N-mer deposited at the ~ 1 mg/h rate typical of the data in Fig. 3 was not the same for this polymer as it was for those prepared by living anionic polymerization. This is very likely a result of the fact that the $M_w = 1200$ g/mol polymer was prepared by free radical polymerization and thus contained different end groups than the $M_w = 600$ g/mol and $M_w = 890$ g/mol polymers.

It is notable that in this particular sample of PS with $M_w = 600$ g/mol we were able to isolate eight different components. These components have T_g values that differ by 63 K. In this particular case we started with 80.1 mg of PS, and after the entire process, we had evaporated 75.7 mg, leaving 4.4 mg of materials with $N \geqslant 14$. The measured T_g value of the remaining component was 304 K. This is greater than any of the components collected for this sample, and so certainly contains mainly N-mers not collected in the previous thermal treatment. Of the 75.7 mg that was evaporated, we successfully collected 70.8 mg for a 94% efficiency. However, our efficiency at producing the pure N-mers is notably less (~ 50%) as this only includes masses that are collected while the resulting T_g is exhibiting a plateau.

According to our calculations of vapor pressure, the vapor pressures of the polymers we are depositing are many orders of magnitude less than the ambient pressure. The fact that at such low temperature there are no other depositing materials, means that we can still successfully deposit even under these conditions. In fact, uniform and constant sample temperature during evaporation is a much more critical factor than low ambient pressure, and having a non-negligible ambient pressure enhances our ability to perform evaporative purification. We note that deposition even at atmospheric ambient pressure is possible, but with reduced efficiency. Tests showed that deposited and remaining materials could be mixed together to reconstitute a material with the same T_g value as the original material. This ability demonstrates that the thermal separation of samples did not result in thermal effects of chain scission, polymerization, or cross linking.

Further use of the data requires that we are able to assign an N value to each of the polymers collected within a particular T_g plateau. To do this we make a comparison to the Fox-Flory relation for $T_g(N)$. While we will later demonstrate the inability of this relation to provide a detailed accurate description of the N dependence of T_g, it should certainly suffice to determine which N corresponds to which T_g. We can also use the evaporated masses in order to find an independent measure of the distribution of N values in each polymer. To do this we consider the amount of mass evaporated at each temperature, rather than the mass deposited (which is shown in Fig. 3). As previously mentioned, the composition of material evaporated is a function of time, and the first material evaporated after a temperature change likely contains a non-negligible fraction of the previous N value. Since we
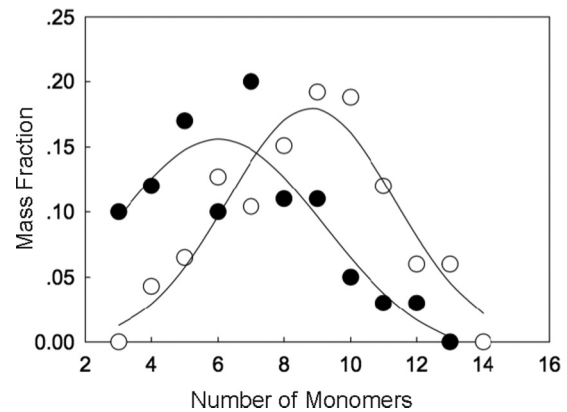

FIG. 4. Distribution of evaporated components during the heating process. The solid symbols are the masses evaporated from the $M_w = 600$ g/mol PS, and the open symbols are the masses evaporated from the $M_w = 890$ g/mol PS. The curves are fits to Gaussian functional forms, and are for illustrative purposes only.

do not know the composition of this first fraction, we include all the masses evaporated at a particular temperature. While this may mistakenly include some of the previous N, it also mistakenly misses some of the correct N that comes off at the higher temperature. If the mass evaporated at the first stage at each temperature was the same, we would expect these effects to almost exactly cancel. For this reason, our process provides a reasonable estimate of the N-mer distribution. The evaporated amounts at each temperature for the $M_w = 600$ g/mol and $M_w = 890$ g/mol material are shown in Fig. 4. For the case of the $M_w = 600$ g/mol PS, there was a significant amount of material that was evaporated at the lowest temperature of 403 K, and we did not separate the monomer and dimer components. From this data we can also calculate the M_w, M_n, and M_w/M_n value of each of the polymers. For the $M_w = 600$ g/mol polymer we calculated $M_n = 571$ g/mol and $M_w = 656$ g/mol with $M_w/M_n = 1.15$. The fact that these are about 10% larger than the quoted values is likely due to our not measuring the monomer and dimer components. For the $M_w = 890$ g/mol PS, we find a $M_w = 916$ g/mol and $M_n = 824$ g/mol for a $M_w/M_n = 1.11$; this is in very good agreement with the quoted values for that polymer. In these calculations we treat the material that had not been evaporated after the full heating process in the following manner. We divide the remaining mass equally among the two N values larger than the last N actually measured (N_{max}) and then denote the volume fraction of all $N > N_{max} + 2$ as zero. We have also used this process to illustrate the masses in Fig. 4. The fact that the T_g value of the remaining material is more than that any of the T_g values of the separated N-mers suggests this is a reasonable representation.

As discussed above, comparison to simulation suggests that the T_g values in each of the plateau's collected come from pure N-mers. Using this same process for each of the starting PS compositions, we can collect what we suspect are pure N-mers for each N from each sample. Since the temperature ranges determine the deposition rates for a particular N-mer, materials prepared in the same manner (with the same end groups) will result in the same N-mers being collected at the same values
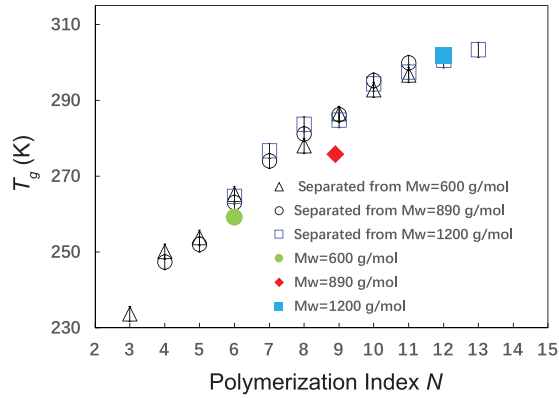
FIG. 5. T_g values of N-styrene as isolated from the three different initial polymers, as well as the T_g values of the initial polydisperse samples.

FIG. 6. T_g values of N-styrene ($N < 10$), and more polydisperse ($N > 10$) polystyrene and fits to Eq. (5) as well as Fox-Flory expressions.

of T. This is indeed what is observed. The T_g values measured in each of the plateaus for the three M_w values considered (600, 890, and 1200 g/mol) are shown in Fig. 5. Also shown in Fig. 5 are the T_g values of the initial polymers with the full distribution of N values.

B. Quantifying T_g as a function of N

The measured T_g values of individual components from each of the starting polymers are provided graphically in Fig. 5. We note that these T_g values show significant deviations from the Fox-Flory relationship [1], and these differences can depend on the polymer chain ends as already noted in Refs. [11,27,28]. In order to understand the deviation from Fox-Flory and provide an alternative functional form for the N dependence of the T_g value, we consider our polymers as a mixture of two components, with weight fractions w_1, w_2, and T_g values T_g^1 and T_g^2, and use the empirical Fox relation for the glass transition temperature of a miscible mixture given by

$$\frac{1}{T_g} = \frac{w_1}{T_g^1} + \frac{w_2}{T_g^2}. \tag{3}$$

In this case we consider one component as the chain; the other is essentially the chain ends. The weight fraction of the chain ends is $\frac{1}{\alpha N}$, and the weight fraction of the chains is $(1 - \frac{1}{\alpha N})$, where the parameter α contains the fact that there are two chain ends and that the weight fraction depends on the relative size of chain ends and chain segments. We can write the T_g value of the chain component as T_g^∞ and the T_g value of the end component as T_g^0. We can substitute this into Eq. (3) to obtain

$$\frac{1}{T_g(N)} = \frac{1/(\alpha N)}{T_g^0} + \frac{1 - 1/(\alpha N)}{T_g^\infty}. \tag{4}$$

We can write this as

$$T_g(N) = \frac{T_g^\infty}{1 + \frac{1}{\alpha N}\left(\frac{T_g^\infty}{T_g^0} - 1\right)}. \tag{5}$$

This is very similar to the procedure used to derive Eq. (7) in Ref. [29] where free volume arguments rather than the Fox relation are used as the starting point. It is interesting
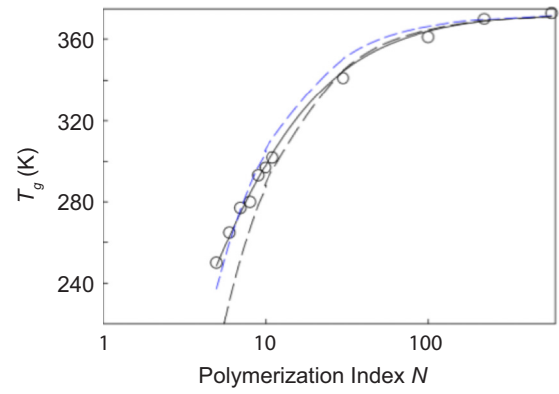
to note that in the case of $N \gg 1$ to first order in $1/N$ we recover the Fox-Flory relationship $T_g(N) \simeq T_g^\infty(1 - A/N)$ where $A = \frac{1}{\alpha}(\frac{T_g^\infty}{T_g^0} - 1)$. Now in the case where N is not large we should use the full Eq. (5) where the only fitting parameter (besides the T_g of bulk large M_w PS) is the combination of physical parameters $\frac{1}{\alpha}(\frac{T_g^\infty}{T_g^0} - 1)$. To make this comparison we use the T_g values from Fig. 5 for N-mers originating from anionically polymerized $M_w = 890$ g/mol polymer, as well as those in Ref. [30] for much larger N (polymers made in the same commercial laboratory and T_g values obtained using the same experimental technique as the present study). Because of the known importance of end groups on measured T_g for small N [27], we restrict ourselves to only one original polymer so that we can be certain that the end groups are the same for all N. The result of this fitting process is shown in Fig. 6. In this case the solid line is the fit to Eq. (5), and the dashed lines are best fit to the common Fox-Flory relationship (blue), and the Fox-Flory relationship with parameters usually employed for larger M_n (black). It is evident that our simple expression provides an excellent, physically motivated fit over the entire range of N (from $N \sim 5$ to $N \to \infty$) with the same number of parameters as the Fox-Flory relation, and to first order in $1/N$ reduces to the commonly used Fox-Flory relation. We note that this same functional form could be used on older collections of (not as monodisperse) low N PS samples [31].

We can also use these results to find a practical upper bound for the largest N value that can be isolated in this technique. We note that we are bounded above in temperature to avoid thermal decomposition. To date, the highest temperature we have worked at is 563 K, which is below the 573 K temperature onset expected for thermal decomposition [20]. At this temperature we can deposit the 13-mer of PS at a maximum rate of about 1 mg/h. If we continue to evaporate at this temperature, we would find that we would eventually exhaust the 13-mer, and deposit the 14-mer, but that would take many hours, and the maximum rate would still only be about 0.01 mg/h. Thus, it seems that avoiding thermal decomposition places an upper bound on the N-mers we can isolate in reasonable quantities *in reasonable time* for the case of PS at 13. However, we should note that for samples with $M_n > 1400$, in addition

to isolating pure N-mers for $N \leqslant 13$ we can significantly reduce the polydispersity of the remaining material. Finally, we note that having the ability to isolate pure N-mers introduces the ability to really study the effect of polydispersity on physical quantities. By mixing the N-mers, we are able to produce samples with arbitrary shaped distributions, and study properties such as T_g, solubility, and mixing properties. The studies are also ideal specimens for recently described samples of atactic PS crystals [32]. The behavior and abundance of such crystals depends strongly on N, so having pure N-mer samples is necessary to develop a detailed understanding. The materials prepared in this paper can also be used to determine the actual vapor pressure values of pure N-mers that had to be calculated for this study. This is important as the calculations we used to guide us do not take into account end group effects at all, and these are clearly important for small N. The same evaporative purification technique has been shown to be able to separate poly(ethylene glycol) into N-mers, and that work will be the subject of a future communication. The technique we described is simple enough to be employed with only slight modification to existing and common vacuum annealing setups, and is readily scalable to larger quantities. Importantly, the technique as described provides a set of N-mers with identical end groups. A variation of the technique could possibly separate polymers with the same N but different end groups.

V. SUMMARY

In summary, we have developed and described a process in order to isolate what appear to be pure N-mers from a polydisperse initial mixture. As far as we know, these N-mer samples represent the PS with the highest degree of monodispersity reported. We have shown that even low-cost samples with an initial M_w/M_n of 1.6 are able to produce the same quality N-mers as those that are produced using polymers produced by living anionic polymerization as the starting material. The T_g values of the separated molecules are well quantified by a simple empirical relationship over the entire range of N. At its most basic level, the technique requires nothing more than clean vacuum and temperature control.

ACKNOWLEDGMENTS

[1] T. G. Fox and P. J. Flory, J. Appl. Phys. **21**, 581 (1950).

[2] S.-J. Li, S.-J. Xie, Y.-C. Li, H.-J. Qian, and Z.-Y. Lu, Phys. Rev. E **93**, 012613 (2016).

[3] D. J. Plazek and V. M. O'Rourke, J. Polym. Sci. **9**, 209 (1971).

[4] V. Marcon and N. F. A. van der Vegt, Soft Matter **10**, 9059 (2014).

[5] T. R. Paxton, J. Appl. Poly. Sci. **7**, 1499 (1963).

[6] S. Napolitano, E. Glynos, and N. B. Tito, Rev. Prog. Phys. **80**, 036602 (2017).

[7] T. M. Beardsley and M. W. Matsen, Phys. Rev. Lett. **117**, 217801 (2016).

[8] M. Szwarc, Nature (London) **178**, 1168 (1956).

[9] S. S. Patil, S. K. Menon, and P. P. Wadgaonkar, Polym. Int. **64**, 413 (2015).

[10] R. P. Lattimer, D. J. Harmon, and K. R. Welch, Anal. Chem. **51**, 1293 (1979).

[11] T. Hatakeyama and M. Seriwaza, Polym. J. **14**, 51 (1982).

[12] K. Ueberreiter and G. Kanig, J. Colloid Sci. **7**, 569 (1952).

[13] K. Ueberreiter and G. Kanig, Z. Naturforsch. A **6**, 551 (1951).

[14] S. Fujishige and N. Ohguri, Makromol. Chem. **176**, 233 (1975).

[15] J. S. Chickos and W. Hanshaw, J. Chem. Eng. Data **49**, 77 (2004).

[16] J. Zhang, C. Con, and B. Cui, ACS Nano **8**, 3483 (2014).

[17] S. Ma, C. Con, M. Yavuz, and B. Cui, Nanoscale Res. Lett. **6**, 446 (2011).

[18] V. Svorcik, V. Rybka, K. Efimenko, and V. Hnatowicz, J. Mater. Sci. Lett. **16**, 1564 (1997).

[19] H. Usui, *Functional Polymer Films* (Wiley-VCH Verlag GmbH and Co. KGaA, Weinheim, Germany, 2011), pp. 287.

[20] M. Guaita, Polym. Int. **18**, 226 (1986).

[21] F. Taylor, Ann. Sci. **5**, 185 (1945).

[22] K. C. D. Hickman, Chem. Rev. **34**, 51 (1944).

[23] I. Langmuir, Phys. Rev. **2**, 329 (1913).

[24] K. J. Laidler and J. H. Maiser, *Physical Chemistry* (Benjamin Cummings, San Francisco, 1982), p 180.

[25] I. C. Sanchez and R. H. Lacombe, J. Phys. Chem. **80**, 2352 (1976).

[26] I. C. Sanchez and R. H. Lacombe, Macromolecules **11**, 1145 (1978).

[27] L. Zhang, J. A. Marsiglio, T. Lan, and J. M. Torkelson, Macromolecules **49**, 2387 (2016).

[28] J. M. G. Cown, Eur. Polym. J. **11**, 297 (1975).

[29] T. G. Fox and S. Loshaek, J. Polym. Sci. **XV**, 371 (1955).

[30] D. Qi, C. R. Daley, Y. Chai, and J. A. Forrest, Soft Matter **9**, 8958 (2013).

[31] L. A. Wall, Roestamsjah, and M. H. Aldridge, J. Res. Natl. Bur. Stand., Sect. A **78A**, 447 (1974).

[32] Y. Chai, Ph.D. thesis, University of Waterloo, 2016.